THE PENNSYLVANIA STATE UNIVERSITY
COLLEGE OF EARTH AND MINERAL SCIENCES

DEPARTMENT OF GEOSCIENCES

Rose Hill Shale Weathering Along a Climosequence in the Appalachian Mountains

A Senior Thesis in Geosciences

by

E. Philip Trowbridge

Submitted in partial fulfillment
of the requirements
for the degree of

Bachelor of Science

Spring 2013

Reviewed and approved by:

5/13/13

Dr. Timothy S. White, Senior Research Associate

Date

5/3/13

Peter J. Heaney, Professor of Geosciences
Associate Head for Undergraduate Programs

Date

Rose Hill Shale Weathering Along a Climate Gradient in the Appalachian Mountains

By: E. Philip Trowbridge

ABSTRACT

Research at Critical Zone Observatories has included the study of soil and the rate at which it forms. In this thesis, chips of Rose Hill Shale were buried along a climosequence in the Appalachian Mountains (in the Susquehanna-Shale Hills Observatory and associated satellite sites) to determine how shale weathers and to begin to quantify weathering and soil formation rates. This study covered only two years of weathering and is part of a longer term experiment. After recovery the shale chips were analyzed for mass loss, physical changes, and elemental chemistry using SEM and EDAX. In the mass loss profiles it was determined that the mass loss of the shale chips was constant through the various soil profiles, except for one depth at each site that displayed elevated mass loss. This increased mass loss may be attributable to a number of factors. Calculated rates of soil formation are not as expected. Slower rates were in the southern sites (TN, and AL), with quicker rates in the northern sites (NY, and VA). The rates that were calculated were averaged at each site and are: in NY 9.15 m/My, in VA 10.19 m/My, in TN 6.87 m/My, and in AL 4.19 m/My.

INTRODUCTION

Soil is an essential resource that is needed to support terrestrial life and feed an increasing global population. The processes that form soil are well understood, but the rates of soil formation are not as well established. While rates of soil erosion are fairly well known, few reliable rates of soil formation exist and those that do are not well quantified and poorly constrained (Amundson, 2004). This lack of information makes it difficult to accomplish long-term management of this important resource.

In agricultural systems, increased erosion rates can be seen due to tillage of cropland. While practices such as no-till and planting cover crops help reduce erosion, occasionally a field has to be tilled to mix the soil. When this happens it disaggregates the soil and erosion rates can increase. Average erosion rates in modern agricultural systems can be greater than 1 mm/yr or 1000 m/My (Montgomery, 2007). This far exceeds the rate at which soil forms. “If agricultural erosion rates remain far beyond the rates of soil production, global society will eventually be compelled to either adopt agricultural methods that sustain the soil or face increasing competition over a shrinking agricultural land base” (Montgomery, 2007). A growing population will only accentuate this problem as we could struggle to feed everyone.

Erosion rates in forested systems are not as extreme as some rates measured in agricultural systems. This is due to the fact that in forests there is vegetative cover year-round holding soil in place. By measuring the ^{10}Be concentration, various studies have calculated long-term erosion rates. One rate that is averaged across all lithologies and provinces in the Appalachian Mountains is 17 ± 9 m/My (Portenga and Bierman, 2011). Another rate measured in the Susquehanna Shale Hills CZO (SSHO) is more specific to our work, as it is a rate of erosion measured on the same shale formation studied in this thesis from the Ridge and Valley

Province, and is 16 ± 5.6 m/My (West et al., 2013). Another study using uranium series disequilibrium models by Ma et al. (2010) calculated an average erosion rate across the SSHO catchment and found a rate of approximately 15 m/My.

The approach in this thesis is to attempt to quantify soil formation rates through an *in situ* shale burial experiment in which the physical and chemical changes are analyzed from Rose Hill Shale chips that have been buried for two years. The results may help estimate a rate of soil formation.

The Critical Zone (CZ) is a relatively new term that describes a system of coupled chemical, biological, physical, and geological processes operating together to support life at Earth's surface (NRC, 2001). Most terrestrial life on Earth is supported by this zone which extends from the outer extent of vegetation down to the lower limits of fresh groundwater (Brantley et al., 2007). Increasing understanding of the complex interactions in the Critical Zone is central to understanding fundamental Earth surface processes and landscape evolution (NRC, 2001). Soil is the central component of the CZ and is the solid interface between gas and water exchange connecting the atmosphere to aquifers (Brantley et al., 2007). To understand the complex interactions that take place in the CZ the U.S. National Science Foundation established Critical Zone Observatories (CZO) in 2007 (Anderson et al., 2008).

The Susquehanna Shale Hills CZO (SSHO) established in the Valley and Ridge province of the Appalachian Mountains in central Pennsylvania is among the first CZOs. The primary focus of the SSHO is to develop a quantitative and predictive understanding of the formation, evolution and structure of shale regolith (NRC, 2001). The site is a forested, temperate-climate catchment developed on shale bedrock (Lin et al., 2006; Jin et al., 2010). This CZO has also incorporated satellite sites on shale bedrock along a climosequence primarily in the Appalachian Mountains and including study sites in Puerto Rico and Wales (Dere et al., 2010).

The CZ can be thought of as a feed-through reactor where the downward advance of the weathering front brings un-weathered rock into the reactor (Anderson et al., 2007). The CZ displays tremendous heterogeneity both vertically and laterally (Anderson et al., 2007). The vertical extent of the CZ reflects the relative rates of downward weathering front advance and erosion from the top (Anderson et al., 2007). Because of these variations, it is a challenge for researchers to be able to quantify a rate of soil formation. These variations reflect chemical and mechanical processes that drive the weathering front into unaltered rock, as well as physical erosion and chemical denudation processes (Anderson et al., 2007). The processes operating in the CZ including tectonic through hill slope to mineral scales all play a large part in determining the chemical weathering rate (Anderson et al., 2007), one of the parameters addressed in this senior thesis experiment. These processes control residence time of material in the CZ, the rate of water flow, the saturation state of water, and the size of rock particles in the regolith, all of which control the chemical weathering flux (Anderson et al., 2007).

The chemical flux varies with depth and is controlled by mineral and weathering solution reactivity and water flow rate (Anderson et al., 2007). Reaction rate is found to increase with water percolation rate, and since water flow rate tends to decrease with depth in the CZ, the chemical weathering rate will decrease with depth (Anderson et al., 2007). Erosion of the weathered material from the top will tend to dampen this decrease, and help make the residence time for rocks in the CZ shorter (Anderson et al., 2007). Because of this some researchers have argued that a shorter residence time of weatherable material, driven by faster erosion, produces faster chemical weathering solute yields (Anderson et al., 2007). Increased chemical weathering leads to increased soil production rates (Heimsath et al., 2012).

This argument contradicts the existing model which indicates that soil production rates are constant for a given climate, and lithology (Heimsath et al., 2012). The Heimsath et al. (2012) study, done in the San Gabriel Mountains in California, presents ^{10}Be estimates of soil production and detrital erosion rates. The researchers averaged erosion rates of catchments on different hill slope angles. Erosion increased as hill slope angle increased. With increased erosion on steep hill slopes little soil cover might be expected, but surprisingly a continuous soil mantle was observed in the Heimsath et al. (2012) study. This strongly demonstrates that soil production rates increase with increasing erosion (Heimsath et al., 2012).

BACKGROUND

Previous rock burial experiments have been accomplished. One particular study was done by Day et al. (1980). In that study, shale disks from a single rock formation were buried in a humid temperate environment (Wales) and a rain forest environment (Malaysia). They also placed disks on wooden trays and left them exposed to the soil surface in Wales and Malaysia. However the air exposed disks were accidently destroyed in Wales. Measuring the mass loss they were able to make the following conclusions.

First, the average mass loss from Wales, excluding the disks in the humic topsoil, was collectively found to be 8.1 mg. The mass loss of the disks in the humic topsoil is 16.1 mg, demonstrating a highly significant difference according to the researchers. In Malaysia the disks were only buried at depths of 20 and 140 cm, and the average mass loss was 28.1 mg. The air exposed disks had a mean loss 18.5 mg. The mass loss plot from this study is shown in Figure 1.

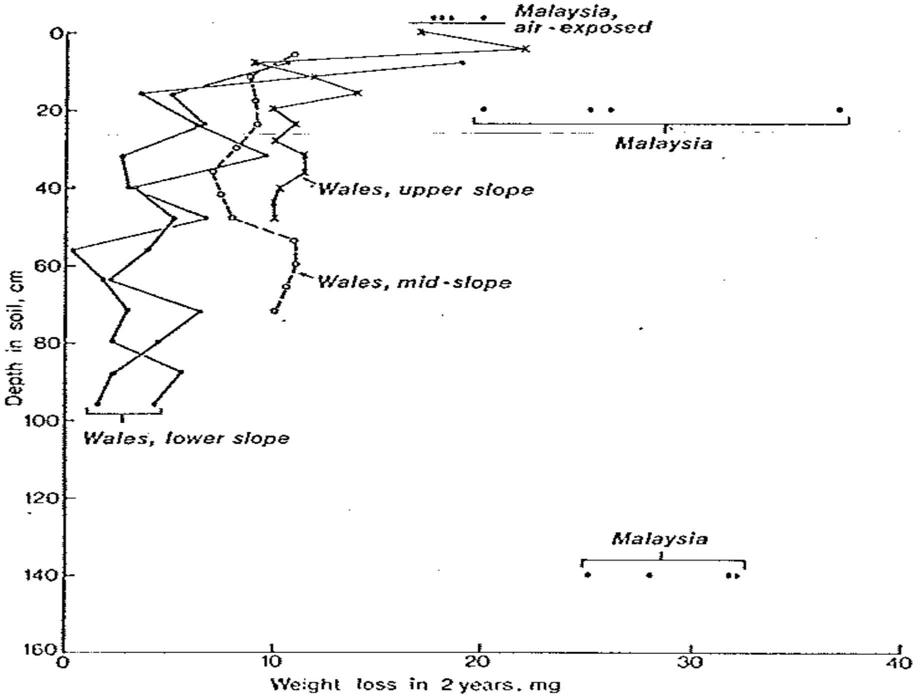

Figure 1: Mass loss plot from Day et al., 1980

The results showed that at the tropical Malaysian site, weathering was 3.5 times faster than at the temperate Wales site. In the humid temperate environment in Wales, the rate of weathering is twice as fast in the humic topsoil as in the lower horizons. Also there may be a slight decreasing trend in weathering with depth on the Wales lower slope. In Malaysia, air exposed disks weather a little slower than the disks buried in the soil.

Another similar study by Thorn et al. (2006) reports their findings of weathering of dolomite, granite, and limestone disks in Sweden. These disks were buried and recovered after 5 and 10 years. They found that the dolomite was the most useful material for monitoring mass loss because the carbonate rock tended to weather rapidly while the granite weathered slowly. The mean total percent mass loss they report for dolomite is 3.90%, for limestone, 7.23%, and for granite, 0.08%. Given these results the researchers suggest that fundamental measures such as soil drainage and pH are clearly dominant factors that dictate mass loss.

A third study was done by Yokoyama and Matsukura (2006) over a 10 year period with granodiorite tablets. The tablets were placed in three different weathering positions: on the ground surface, above an aquifer, and in an aquifer. The tablets experienced mass losses of 0.022 wt% yr^{-1} for the ground surface, 0.013 wt% yr^{-1} above the aquifer, and 0.42 wt% yr^{-1} in the aquifer. These results show that the tablet in the aquifer was remarkably weathered compared to the tablets above the aquifer and on the surface. To evaluate the amount of chemical weathering on the tablet, they ran a laboratory dissolution experiment and obtained rates that were approximately 50 times slower than the field rate in the aquifer. They concluded that physical weathering processes in the field are large compared to the chemical process.

Rhyolite disks were also studied over a 5 year period by Matsukura et al. (2001). Here, two kinds of rhyolite, one that is 2,600 years old and a second that is 20,000 years old, were buried, exhumed, washed, weighed, and reburied every three months. The results show that the older rhyolite had a higher rate of chemical weathering than the younger rhyolite.

METHODS

Field Methods:

The study sites correspond to those considered by A. Dere, a Ph.D. candidate in Geosciences (Dere et al., 2013), and are listed from highest latitude to lowest latitude: Chadwicks, New York (NY); Whipple Dam State Park and SSHO, Pennsylvania (PA); Goshen National Wildlife Management Area, Virginia (VA), Big Ridge State Park, Tennessee (TN); Lake Guntersville State Park, Alabama (AL). These sites are shown in figure 2.

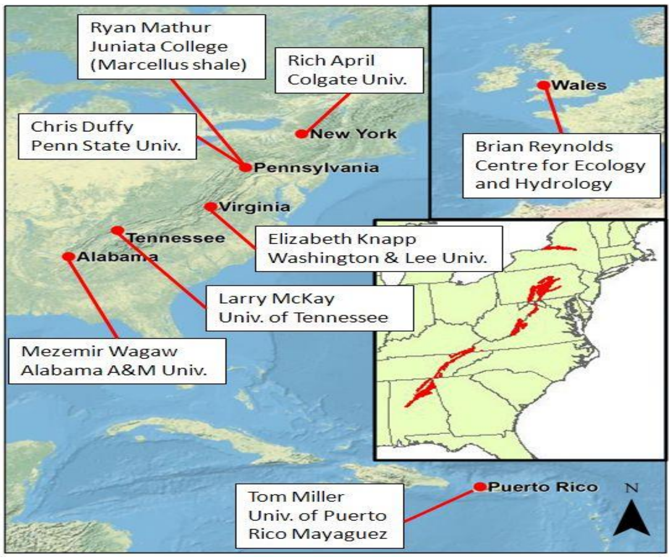

Figure 2: Map of transect sites used in this experiment.

The potential variability of parent material bedrock was limited by choosing sites located on Silurian iron-rich, organic-poor Clinton Group shale, known as the Rose Hill Formation in NY (Gillette, 1947), PA (Fleckinger, 1969) and VA (Kozak, 1965), the Rockwood Formation in TN (Pratt, 1964),and the Red Mountain Formation in AL (Sanford, 1966). Forested sites were chosen to minimize potential biotic variability.

The source of the shale chips is from a single outcrop of Rose Hill Shale near Reedsville, PA. The outcrop was hammered into about 5 cm to get fresh un-weathered rock. A 10 cm by 10 cm section of the Rose Hill Shale was then taken and hammered into the shale chips that were buried across the transect for this study.

The shale chips were weighed and sewn into mesh bags. The bags were made of two squares of approximately 5 cm by 5 cm that were sewn together. The mesh size is 1 cm^2. Nylon tags with the sample number were sewn onto the bags. Nylon string was tied to the bags and gathered into a PVC pipe to minimize exposure and brought to the surface of the soil pit.

The shale chips were buried in soil pits across the climosequence. The soil pits were dug for other research purposes and the shale chips were inserted laterally into the wall of the pit by making small holes using a putty knife. Three shale chips were buried at each depth to improve accuracy so that an average could be obtained. In NY the chips were buried at depths of 5, 25, 60, 85, 125, and 175 cm. In PA there is only one depth at 10 cm because of shallow soils. In VA the depths are 5, 15, 30, 45, 55, and 90 cm. In TN the depths are 15, 30, 50, 75, 100, and 140 cm. In AL the depths are 10, 30, 50, 65, 90, and 130 cm. After being buried the sites were marked and excavated and brought back to the Penn State lab after 2 years. Figure 3 shows some pictures of the shale before and after burial, as well as the chips being buried and recovered.

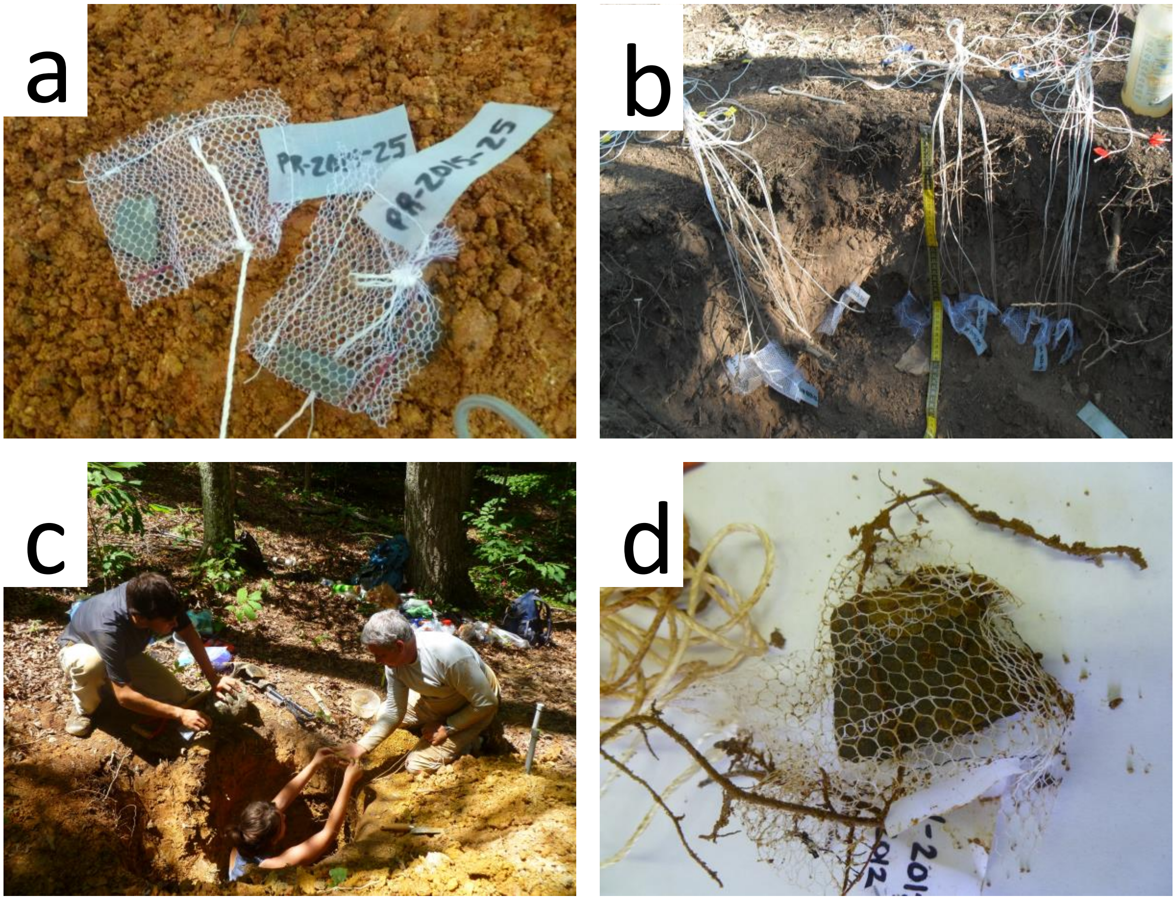

Figure 3: a) Shale chips in mesh bags prior to burial; b) shale burial in the walls of a soil pit in Virginia; c) excavation of buried shale chips in TN; d) a recovered shale chip from New York after 2 yr of burial. Note roots growing through mesh bag.

Lab Methods:

Mass Loss

Once shale chips were recovered and returned to Penn State they were removed from the mesh bags and washed with deionized water through a sieve so no broken fragments were lost. The shale chips were then dried and weighed to obtain a mass loss for each chip. Excel was used to manage the data and construct mass loss plots for each site. In constructing the mass loss plots we excluded the chips that had gained mass and chips that had more than 70 mg of mass loss. Some of the shale chips were shattered into tiny pieces so it is possible that the higher mass loss can be accounted for by loss of some pieces during recovery and processing.

EDAX Geochemistry

The shale chips were observed under a scanning electron microscope (SEM) and were analyzed for chemistry using Energy Dispersive Analysis of X-rays (EDAX). EDAX works by sending a high energy beam of particles focused into a target sample. The beam may excite electrons in an inner energy shell causing them to be ejected from the shell. An electron from an outer shell will fill the hole in the lower shell. The difference in energy between the high and low shell may be released in the form of an X-ray. The number and energy of the X-rays emitted can be measured and are characteristic for each element, allowing for elemental composition to be measured (Goldstein, 2003). We selected one shale chip from each depth at each site and analyzed 3 spots on each chip. The elements that were analyzed using EDAX are O, Na, Mg, Al, Si, Zr, K, Ba, Ti, Mn, and Fe. The scanning energy for EDAX analysis was from 0 to 20.00 keV with an elapsed time of 100 s. The accuracy of the EDAX system is +/- 0.2% however this assumes a flat homogenous sample. Shale geochemistry may vary somewhat between chips due to natural variations between laminations in the formation though we minimized this by splitting chips from a single piece obtained from one outcrop. The lack of flat surfaces on the chips may have increased error in the determinations presented here. Also error can rise when looking for lighter elements such as Na. In Excel the chemistry for each element was averaged and Tau plots were constructed with Ti as the immobile element.

Tau Plots:

A chemical mass balance model is used to quantify elemental losses and gains from chemical weathering in the soil (Brimhall and Deitrich, 1987). This model is predicated on the characterization of a parent material, which in this case is the Rose Hill Shale. The term that is used to quantify the mass balance model is the element mass transfer coefficient, or tau (Anderson et al., 2002). The equation that is used is as follows:

$$\tau_{i,j} = \frac{C_{j,w}\, C_{i,p}}{C_{j,p}\, C_{i,w}} - 1$$

Here, τ is a dimensionless coefficient representing the ratio of the concentration, *C,* of an element of interest (*j*) relative to an immobile element (*i*) in the weathered soil (*w*) and the parent (*p*) (Brimhall and Dietrich, 1987; Anderson et al., 2002). This approach measures the relative changes in concentration of the elements of interest or mobile elements, compared to the immobile element that is not involved in weathering. When $\tau = 0$, element *j* is neither enriched nor depleted with respect to element *j* in the parent; when $\tau < 0$, the element has been lost relative to immobile element *i* in parent and $\tau > 0$ indicates the element has been added to the profile relative to parent (Brantley and White, 2009).

The parent material that was used to calculate tau is un-weathered Rose Hill shale. Four parent rocks were analyzed but the chemistry of the fourth rock is excluded from the averages because it had anomalously high Fe concentrations compared to the other three rocks.

RESULTS

Mass Loss Plots:

The mass loss plots show that there is not much variation with depth overall, though in each plot there is one depth where the mass loss is significantly higher than the rest. In NY the average mass loss is about 20 mg. At 60 cm depth the mass loss is higher at about 42 mg. The mass loss at 10 cm in PA was very scattered as 2 shale chips had gained mass and the third has a mass loss of 720 mg. At the VA site the average mass loss is about 20 mg. The data here is inconclusive however because a lot of the shale chips recovered were shattered and show extremely high mass loss or net mass gain. Net mass gain is unlikely over the time scale of two years because the shale chips are weathering in the soil and should therefore have lost mass. In TN the mean mass loss is about 10 mg. At 50 cm the mass loss is higher than the other depths, at 38 mg. The mass loss at the AL site is 8 mg through the profile. There is a jump in the mass loss at 30 cm depth where the mass loss is about 22 mg.

EDAX Geochemistry Plots:

These plots show the concentrations of the elements analyzed with depth. In these plots the concentrations of Na, Mg, and Ti are relatively constant and do not change very much with depth in any of the profiles. One trend visible in these plots is that increases in Fe concentration correspond to decreases in the concentration of Si. For example in NY we see the concentration of Fe increase at 25 cm depth and then decrease to 85 cm depth. The Si concentration shows the opposite, where the concentration decreases at 25 cm and then increases to 85 cm. Al and K display little variation, staying around 13.5 weight percent and 5 weight percent respectively. These plots are shown below in figure 4

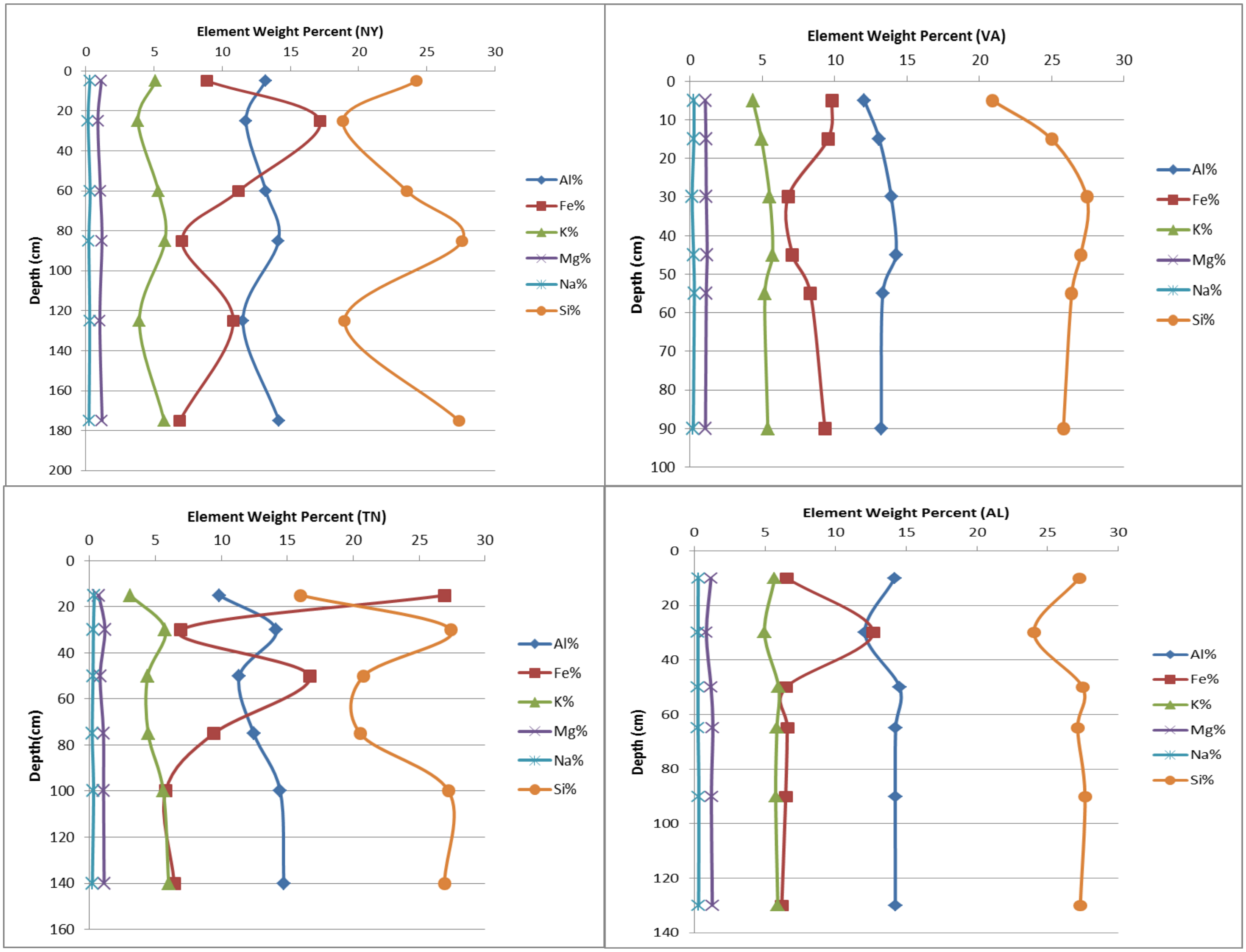
Element Weight Percent (NY)

Element Weight Percent (VA)

Element Weight Percent (TN)

Element Weight Percent (AL)

Figure 4: Clockwise from top left is NY, VA, AL, and VA. These plots show the element concentrations with depth.

Tau Plots:

Using the chemical mass balance model to calculate tau plotted by depth, the following results can be observed. In the NY plot we see an addition, depletion, addition profile for Al, Mg, K, Na, and Si. The addition that we see is at 90 cm depth. Fe is enriched through the whole profile. In VA, depletion of Al, Mg, K, Na, and Si is visible from 10-50 cm. At 50-60 cm there is some addition and then below 60 cm these elements are depleted. Fe is enriched through the profile with some addition at 30 cm. In TN there is depletion of K and Mg from 0-60 cm and some addition from 60-100cm. Below 100 cm Mg is depleted and K shows little depletion or addition. Al, Fe, and Na are all enriched through the profile with Na showing possible depletion below 110 cm. Si doesn't change and has little variation through the profile. In AL, Fe addition is observable down to 30 cm with depletion of Mg, K, Si, and Al down to 60 cm. Na is depleted down to 90 cm. All elements show little change below 90 cm down to the depth of soil at 130 cm. Mn and Ba were not included in the tau plots because they exhibited peculiar behavior. The mass loss plots are shown alongside the tau plots below in figure 5.

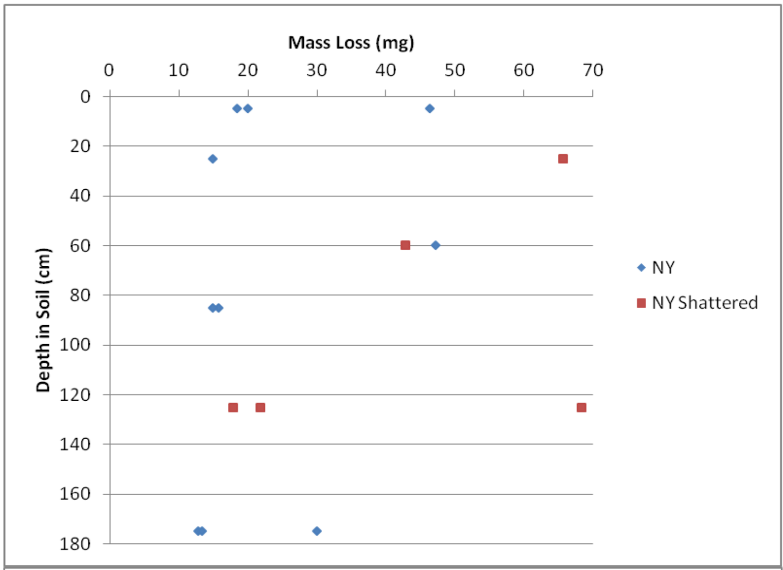

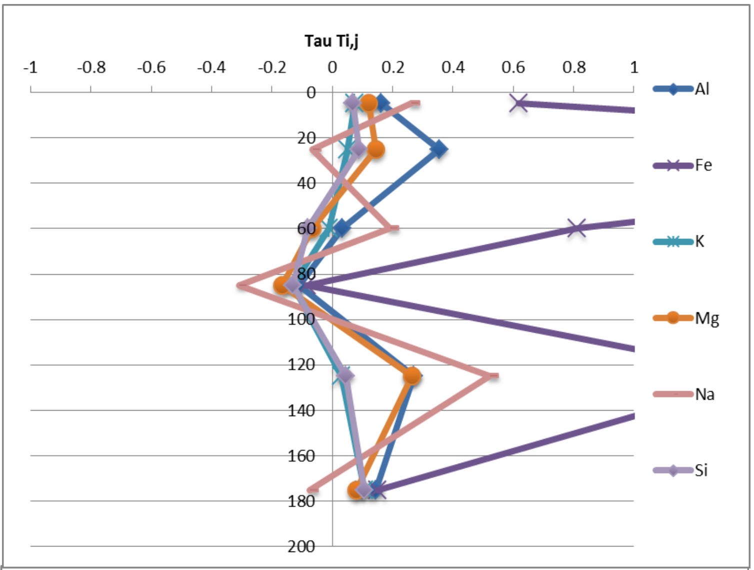

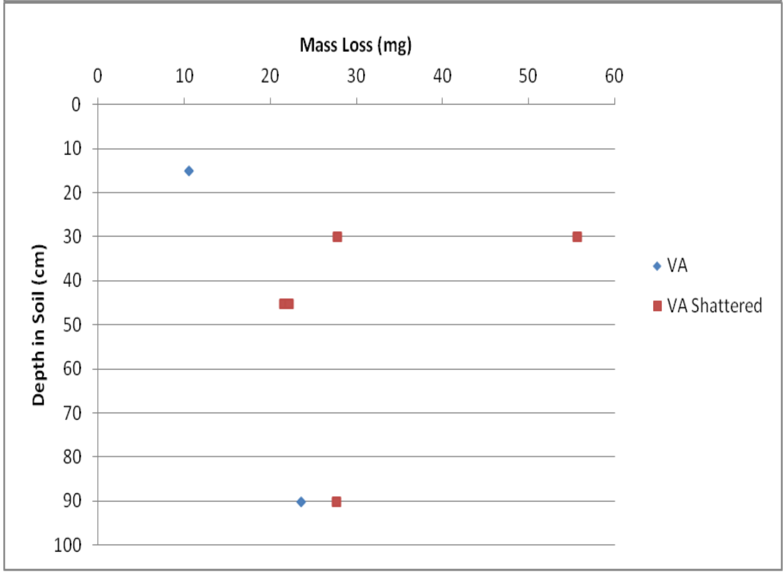

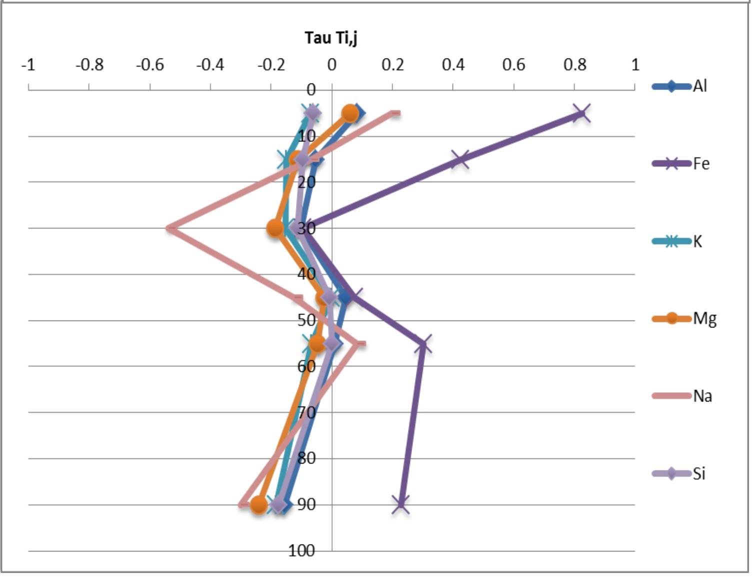

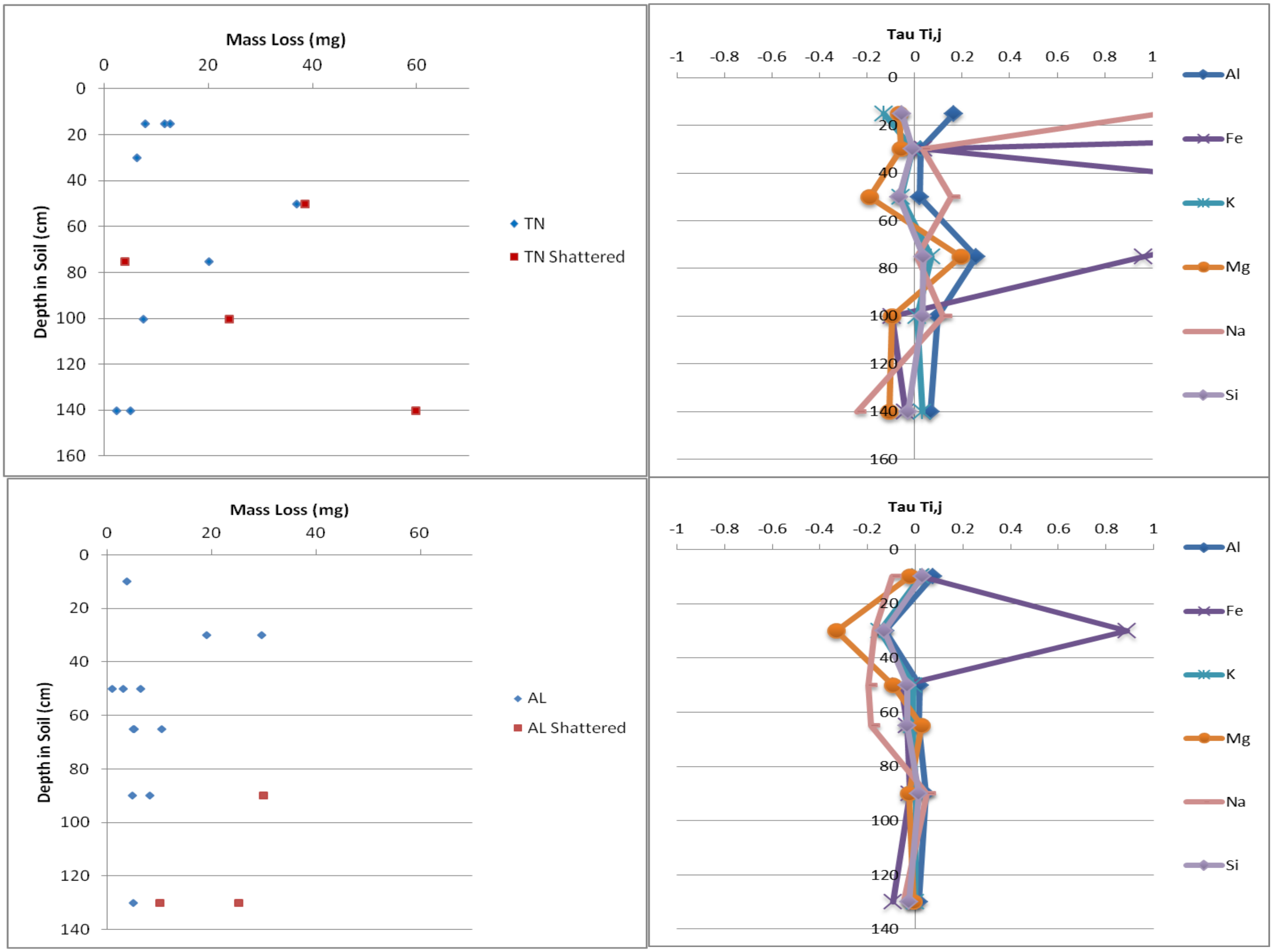

Figure 5: From the top to bottom there is NY, VA, TN, and AL. The mass loss plots alongside the tau plots.

DISCUSSION

The following observations can be made through comparing the mass loss and tau plots. First, one might expect the horizon that exhibits the most mass loss to correspond to higher depletion in the tau plots. In AL this is the case, where the mass loss is greatest at 30 cm and in the tau plot all the elements with exception of Fe are depleted there. A similar observation can be made in VA where all the elements are depleted at the horizon of highest observed mass loss, also at 30 cm. However this is not the case across all of our sites. In TN, this observation is valid, but far less magnitude. In NY the depletion of elements in the tau plot is present, but the depletion is below the horizon of greatest mass loss.

The mass loss data observed in our Appalachian study sites is similar to the Day et al. (1980) study, though the weathered chips studied in this thesis display more mass loss than the experiment in Wales, likely attributable to the lower Mean Annual Temperature (MAT) in Wales. In Wales greater mass loss was observed soil horizon, likely due to the presence of an organic soil horizon where organic acids are able to more effectively weather the shale. This prominent organic soil horizon is not present in the Appalachian study sites. The average mass loss in Wales was 8.1 mg, but 16.1 mg in the organic horizon. In Malaysia the average mass loss was 28.1 mg. The average mass loss in NY and VA is 20 mg, in TN, 10 mg, and in AL, 8 mg. These values are comparable and could be explained by the latitudinal variations in MAT as the greatest mass loss is in Malaysia (lowest latitude) and low mass loss in Wales (highest latitude), with the Appalachian sites falling more or less in between.

The mass loss plots in this study show one horizon where the mass loss is greater at each site. In NY this could be due to the fact that the study site is in a coniferous forest. Here the soil is classified as a spodosol and with an organic acid layer, similar to that in Wales, leading to more intense chemical weathering and greater mass loss. In VA and TN the increased mass loss is just above zones of redoximorphic features in the soil profile, while in AL the increased mass loss is 30 cm above where redoximorphic features are observed – suggesting a relationship between seasonal variations in soil moisture content, chemical weathering and mass loss. As water percolates through the soil column it gradually approaches chemical equilibrium with host material and thus reacts less as it progresses along a subsurface pathway. This explains why at greater depths in the soil less mass loss is observed.

Elemental Depletion:

Integration of tau plot curves provides a mechanism to calculate mass loss in the shale that is due to a particular element, a method described in Brantley and Lebedeva (2011). The equation is:

$$\mathrm{M}j = \rho_p C_{j,p} \int_0^L \frac{\tau_j(z)}{(\varepsilon_i(z) + 1)} dz$$

Here, z is the depth at which the shale chips were buried, M_j is the total mass loss of element *j* from the shale chip, ρ_p is the density of the parent rock, $\mathrm{C}_{\mathrm{j,p}}$ is the concentration of element *j* in the parent rock.

Based on work by Dere et al. (2013) it appears that Na is one of the first elements to weather out of rock, likely from feldspar, thus we have chosen to calculate a mass balance based on Na. Due to the high levels of depletion of Mg in the studied profiles, we also include Mg in the mass balance calculations that follow. The VA and AL profiles show the strongest relationship between mass loss and the tau plots. In these profiles Na shows the most depletion through the profile, while Mg is the next most depleted element. The calculations also include the other major elements across all sites and are shown in Table 1.

AL	Ti					
	(tau*deltaZ)					
Depth (cm)	Al	Fe	K	Mg	Na	Si
10.0	0.741453	0.218376	0.216491	-0.20665	-0.97522	0.313461
30.0	-2.53256	17.75785	-2.96041	-6.6129	-3.44828	-2.61216
50.0	0.403951	-1.18932	-0.11175	-1.83263	-3.92804	-0.69213
65.0	0.228569	-0.50778	-0.16971	0.375356	-2.76876	-0.49329
90.0	1.094977	-0.53166	0.073019	-0.64455	1.253918	0.38797
130.0	0.552481	-3.65163	-0.04556	-0.2704	-1.94726	-1.04452
sum	0.48887	12.09583	-2.99793	-9.19178	-11.8136	-4.14067
VA	Ti					
	(tau*deltaZ)					
Depth (cm)	Al	Fe	K	Mg	Na	Si
5.0	0.413652	4.12473	-0.35523	0.303166	0.989783	-0.30009
15.0	-0.52822	4.26009	-1.49742	-1.12903	-0.68966	-0.95514
30.0	-1.50304	-1.41973	-2.26885	-2.78871	-8.06897	-1.69696
45.0	0.701059	1.137723	-0.03481	-0.38673	-1.87304	-0.10879
55.0	0.097571	3.03508	-0.66642	-0.45993	0.829741	-0.0009
90.0	-5.462	8.031331	-6.42834	-8.37489	-10.5286	-6.17645
sum	-6.28098	19.16922	-11.2511	-12.8361	-19.3407	-9.23833
NY	Ti					
	(tau*deltaZ)					
Depth (cm)	Al	Fe	K	Mg	Na	Si
5.0	0.804434	3.093899	0.378032	0.599707	1.30094	0.346073
25.0	7.125973	61.88412	1.031883	2.899386	-1.29721	1.758494
60.0	1.125764	28.43339	-0.36728	-2.36277	6.735261	-2.80154
85.0	-2.7588	-2.07617	-3.24675	-4.1239	-7.74742	-3.27823
125.0	10.77227	58.41962	1.200125	10.59384	20.90909	1.825418
175.0	7.206946	7.502491	5.256741	4.032258	-3.7931	5.267728
sum	24.27658	157.2573	4.252752	11.63852	16.10756	3.117934
TN	Ti					
	(tau*deltaZ)					
Depth (cm)	Al	Fe	K	Mg	Na	Si
15.0	0.358177	0.560538	-0.15491	-0.84677	0.517241	-0.10854
30.0	0.311746	31.43041	-0.87349	-2.84274	2.327586	-1.00127
50.0	5.16944	19.26694	1.381956	3.864247	0.215517	0.735498
75.0	2.402824	-2.42725	0.225904	-2.4162	2.976832	0.793121
100.0	1.664255	-0.9716	0.817556	-2.62097	-6.03448	-0.66027
140.0	0	0	0	0	0	0
sum	9.906442	47.85904	1.397017	-4.86244	0.002694	-0.24146

Table 1: Elemental depletion (g/m^2) calculated from tau plot

Fe results:

The Fe results present a problem because using the mass balance model equation it is enriched throughout the profiles with respect to the parent material. One explanation for the enrichment of Fe is due to the presence of iron coatings on the rock and oxidation. EDAX analysis cannot analyze the whole rock so the iron coatings could give the appearance that Fe is enriched when in reality if whole rock geochemistry was applied no enrichment may have been observed.

Weathering Rates:

The weathering rates were calculated by assuming the area of each chip to be 5 cm^2 with a bulk density of 2.65 g/cm^3.

$$\frac{mass\ loss\ (mg)}{2\ years\ for\ chip} x \frac{1\ g}{1000\ mg} x \frac{cm^3}{2.65\ g} x \frac{1\ chip}{5\ cm^2} x \frac{1\ m}{100\ cm} x \frac{1000000\ years}{My} = \frac{m}{My}$$

Using these values and the measured mass loss a weathering rate was calculated. In calculating the average weathering rate, two categories of chips were not included in the average: first one, any chips that displayed mass gain over the two years, and second, any chips that displayed anomalously high mass loss (from the chips being shattered) based on comparison with replicates. Since MAT increases from north to south along the transect, the average weathering rate in AL might be expected to be the highest while NY would be lowest. However this was not what we observed in this experiment. VA had the highest weathering rates in this experiment and AL had the lowest calculated weathering rate.

Weathering Rates	NY	VA	TN	AL
m/My	9.15	10.19	6.87	4.19

The calculated weathering rates from the measured mass loss range from 10.2 to 4.2 m/My of soil production. Averaged erosion rates across the Appalachian Mountains are 17 ± 9 m/My. This rate was found by Portenga and Bierman (2011) and includes erosion rates across all lithologies and provinces in the Appalachians. Specifically in the SSHO, a measured erosion rate on shale is 16 ± 5.6 (West et al., 2013). Our calculated weathering rates from this study are less than calculated erosion rates, suggesting that these Appalachian shale soils are subjected to net long-term loss.

Considering NOAA weather data obtained from near the study sites we find that NY had more precipitation over the duration of the experiment than normal. Since water is a big driver of weathering, this may explain why NY shows a relatively high calculated weathering rate. In AL the temperature data is lower over the weathering period than normal by about 5 degree Celsius. This may account for the low weathering rate that was calculated. In general, 2011 was a relatively wet year, an observation that may suggest that the calculated weathering rates from this experiment are higher than long-term averages.

New York	**Precipitation**	**Temperature**		**Virginia**	**Precipitation**	**Temperature**
year	**cm**	**degree (C)**		**year**	**cm**	**degree (C)**
2012	102.8192	9.1		2012	92	11.3
2011	133.35	8.4		2011	132	11.4
2010	130.048	8.7		2010	91	10.6
Average	122.0724	8.7			105	11.1
Long Term Average	106	8.3			106	11.0
Tennessee	**Precipitation**	**Temperature**		**Alabama**	**Precipitation**	**Temperature**
year	**cm**	**degree (C)**		**year**	**cm**	**degree (C)**
2012	102	14.6		2012	122	11.3
2011	168	13.6		2011	172	11.4
2010	136	12.9		2010	120	10.6
Average	135	13.7			138	11.1
Long Term Average	138	14.0			136	16.0

Future Work

This thesis study will serve as a baseline for comparison the shale chips that will exhumed in 5 and 10 years. The longer term data from these future experiments will help to eliminate the sporadic short-term effects of abnormal years where the weather is wetter or cooler than usual. In the 5 and 10 year chips accelerated rates of soil formation might be expected because as minerals begin to weather, new fresh surfaces are exposed, increasing the surface area of the rock, thereby increasing the weathering rate. The inclusion of data from 5 and 10 years into the experiment will provide a more accurate means to calculate weathering rates.

CONCLUSION

Elemental depletion, calculated from the tau plots show that Na is among the first elements to weather out rock due to feldspar weathering. The weathering rates that we calculated in this study, although opposite of what might be expected, are less than modern calculated rates of erosion. However, these weathering rates could be the way they because of abnormal weather over the duration of the experiment. The results presented here are based on only two years of weathering, the beginning of a longer term experiment. The results of the longer term experiment may provide information for predicting the impact of climate change on soil production. The next phase of the experiment should also include whole rock elemental analyses to assess the potential error that is present from using the EDAX system.

ACKNOWLEDGEMENTS

I would like to thank my advisor Dr. Tim White for all his help on this project as well as Ashlee Dere, a Ph.D. candidate in Geosciences. Also, thanks to Scott Kralik for his assistance with SEM and EDAX, and Dr. Peter Heaney for preparing us to write this thesis. Funding for this project came from the Penn State Geosciences Department and the National Science Foundation award to the Susquehanna-Shale Hills CZO.

References

Amundson R. (2004) Soil formation. In *Treatise in Geochemistry* (eds. J. I. Drever, H. D. Holland , and K. K. Turekian.). Elsevier, Amsterdam. pp. 1-35.

Anderson S. P., Bales R. C., Duffy C., J. (2008) Critical Zone Observatories: Building a Network to Advance Interdisciplinary Study of Earth Surface Processes. *Mineralogical Magazine* **72(1)**, 7 – 10.

Anderson S. P., Blanckenburg F., White A. F. (2007) Physical and Chemical Controls on the Critical Zone. *Elements* **3**, 315 – 319.

Anderson S. P., Dietrich W. E. and Brimhall G. H. (2002) Weathering profiles, mass-balance analysis, and rates of solute loss: Linkages between weathering and erosion in a small, steep catchment. *GSA Bulletin* **114**, 1143-1158.

Brantley S. L. and Lebedeva M. (2011) Learning to Read the Chemistry of Regolith to Understand the Critical Zone. *Annual Review of Earth and Planetary Sciences* **39**, 387-416.

Brantley S. L. and White A. F. (2009) Approaches to modeling weathered regolith. *Rev. Mineral. Geochem.* **70**, 435-484.

Brantley S. L., Goldhaber M. B. and Ragnarsdottir K. V. (2007) Crossing disciplines and scales to understand the critical zone. *Elements* **3**, 307–314.

Brimhall G. H. and Dietrich W. E. (1987) Constitutive mass balance relations between chemical composition, volume, density, porosity, and strain in metasomatic hydrochemical systems: Results on weathering and pedogenesis. *Geochim. Cosmochim. Acta* **51**, 567-587.

Day M. J., Leigh C., and Young A. (1980) Weathering of rock discs in temperate and tropical soils. *Z. Geomorph. N.F.* 11-15.

Dere, A. L., White T. S., April R. H., Reynolds B., Miller T. E., Knapp E. P., McKay L. D. and Brantley S. L. (2012) Climate dependence of feldspar weathering along a latitudinal gradient. Geochim. Cosmochim. Acta. In review.

Dere A. L., White T., Jin L., Harbor D., Townsend M., Brantley S. L. (2010) Shale Weathering Rates Across a Continental – Scale Clomosequence. World Congress of Soil Science, Soil Solutions for a Changing World. Published on CDROM.

Heimsath A. M., DiBiase R. A., and Whipple K. X. (2012) Soil production limits and the transition to bedrock – dominated landscapes. *Nature Geoscience*. **5** 210-214.

Jin L., Ravella R., Ketchum B., Heaney P. and Brantley S. L. (2010) Mineral weathering and elemental transport during hillslope evolution at the Susquehanna/Shale Hills Critical Zone Observatory. *Geochim. Cosmochim. Acta*. **74**, 3669-3691.

Joseph Goldstein (2003). *Scanning Electron Microscopy and X-Ray Microanalysis*. Springer. ISBN 978-0-306-47292-3. Retrieved 12 April 2013.

Lin H. (2006) Temporal stability of soil moisture spatial pattern and subsurface preferential flow pathways in the Shale Hills Catchment. *Vadose Zone J.* **5**, 317-340.

Ma L., Chabaux F., Pelt E., Blaes E., Jin L. and Brantley S. (2010) Regolith production rates calculated with uranium-series isotopes at Susquehanna/Shale Hills Critical Zone Observatory. *Earth Plan. Sc. Lett.* **297**:211- 225.

Matsukura Y., Takashi H., Chiaki T. O. (2001) Rates of chemical weathering of porous rhyolites: 5 – year measurements using the weight loss method. *Catena* **43**, 341-347.

Montgomery D. R. (2007) Soil erosion and agricultural sustainability. *Proceedings of the National Academy of Sciences of the United States of America* **104**, 13268-13272.

National Research Council (NRC) (2001) Basic Research Opportunities in Earth Science. National Academy Press, Washington, 154 pp.

Portenga E. W. and Bierman P. R. (2011) Understanding Earth's eroding surface with 10984 Be. GSA Today 21:4-10.

Thorn C. E., Dixon J.C., Darmody R.G., and Allen C. E. (2006) Ten years (1994-2004) of 'potential' weathering in Karkevagge, Swedish Lapland. *Earth Surface Processes and Landforms* **31**, 992-1002.

West, N., Kirby E., Bierman P., Slingerland R., Ma L., Brantley S. and Rood D. (2012) Regolith transport on hillslopes in the Susquehanna Shale Hills Critical Zone Observatory inferred from meteoric 10Be. J. Geophys. Res-Earth. In review.

Yokoyama T. and Matsukura Y. (2006) Field and laboratory experiments on weathering rates of granodiorite: Separation of chemical and physical processes. *Geology* **34**, 809-812.